Computers and Concrete, *Vol. 22, No. 4 (2018) 383-393*
DOI: https://doi.org/10.12989/cac.2018.22.4.383

Experimental study on RC frame structures strengthened by externally-anchored PC wall panels

Seung-Ho Choi[1a], Jin-Ha Hwang[1b], Deuck Hang Lee[2c], Kang Su Kim[*1], Dichuan Zhang[2d] and Jong Ryeol Kim[2e]

[1]*Department of Architectural Engineering, University of Seoul, 163 Siripdaero, Dongdaemun-gu, Seoul, 02504, Korea*
[2]*Department of Civil Engineering, Nazarbayev University, 53 Kabanbay Batyr Ave., Astana, 010000, Republic of Kazakhstan*

(Received February 8, 2018, Revised October 3, 2018, Accepted October 11, 2018)

Abstract. Infill wall strengthening method has been widely used for seismic strengthening of deteriorated reinforced concrete (RC) frame structures with non-seismic details. Although such infill wall method can ensure sufficient lateral strengths of RC frame structures deteriorated in seismic performances with a low constructional cost, it generally requires quite cumbersome construction works due to its complex connection details between an infill wall and existing RC frame. In this study, an advanced seismic strengthening method using externally-anchored precast wall panels (EPCW) was developed to overcome the disadvantage inherent in the existing infill wall strengthening method. A total of four RC frame specimens were carefully designed and fabricated. Cyclic loading tests were then conducted to examine seismic performances of RC frame specimens strengthened using the EPCW method. Two specimens were fully strengthened using stocky precast wall panels with different connection details while one specimen was strengthened only in column perimeter with slender precast wall panels. Test results showed that the strength, stiffness, and energy dissipation capacity of RC frame specimens strengthened by EPCWs were improved compared to control frame specimens without strengthening.

Keywords: earthquake engineering; reinforced concrete; RC frame; RC wall; strengthening

1. Introduction

According to several post-earthquake investigations, a great number of low and medium rise reinforced concrete (RC) buildings have been severely damaged, and there were heavy casualties especially in the school buildings (Baran and Tankut 2011). In response, various seismic assessment and strengthening methods have been proposed for low and medium rise seismically-deficient RC buildings (Sahoo and Rai 2010, Bailey and Yaqub 2012, Kabeyasawa *et al.* 2009, MOE and KIEE 2011, Meshaly 2014, Lee *et al*. 2013, Karantoni 2013, Karaca *et al*. 2017, Lin *et al*. 2017, Bas *et al*. 2017, Motezaker and Kolahchi 2017), and many researches have been conducted regarding the cast-in-place RC and precast concrete (PC) infill wall strengthening methods (Kahn and Hanson 1979, Frosch 1996 and 1999, Matsumoto 1998, Yun *et al*. 2006, Almusallam and Al-Salloum 2007, Ozden *et al*. 2011, Baran and Tankut 2011, Koutas *et al*. 2015, Tesser and Talledo 2017). Frosch (1999) proposed a multi precast panel strengthening method using shear key connections to improve the constructability of the existing infill wall system and to ensure economic efficiency. Yun *et al*. (2006) proposed a strengthening method for RC frame structures with non-seismic details using infill walls made of the strain-hardening cement composites, and Almusallam and Al-Salloum (2007) investigated the behavior of fiber-reinforced polymer (FRP) strengthened infill walls. Kim *et al*. (2009) examined the effect of notches placed in the middle of infill walls to control and minimize damages accumulated to the existing frame structures. Baran and Tankut (2011) also proposed a seismic strengthening method using precast concrete panels, in which they utilized the epoxy mortars to improve their compressive strengths. Ozden *et al*. (2011) suggested a unique strengthening method of RC frames by utilizing CFRP hollow clay tiles. In recent years, Koutas *et al*. (2015) conducted a study on the seismic strengthening of masonry-infilled frames with the textile-reinforced mortars. Lee *et al*. (2009) pointed out that some seismic retrofitting methods to improve the ductility of a whole structural system is not efficient for medium and low rise existing RC structures with non-seismic details due to their insufficient lateral shear resistances, and it was emphasized that a strength enhancement method can be a better way for an efficient seismic strengthening, such as the shear wall-type strengthening method.

According to the afore-mentioned studies, the concrete

∗Corresponding author, Professor
E-mail: kangkim@uos.ac.kr
[a]Ph.D. Candidate
E-mail: ssarmilmil@uos.ac.kr
[b]Ph.D.
E-mail: jinhahwang@uos.ac.kr
[c]Professor
E-mail: deuckhang,lee@nu.edu.kz
[d]Professor
E-mail: dichuan,zhang@nu.edu.kz
[e]Professor
E-mail: : jong,kim@nu.edu.kz

ISSN: 1598-8198 (Print), 1598-818X (Online)

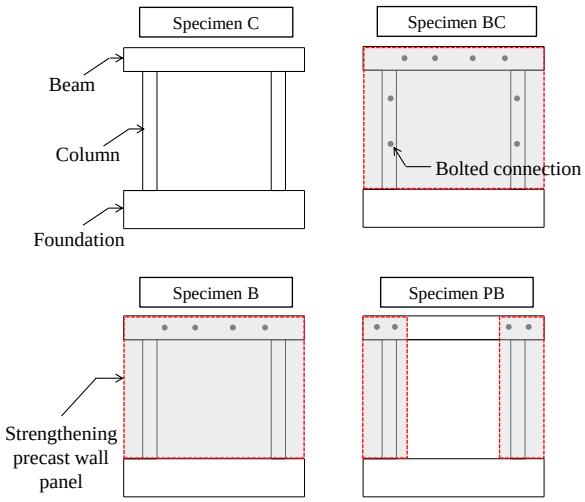

Fig. 1 Description of key test variables

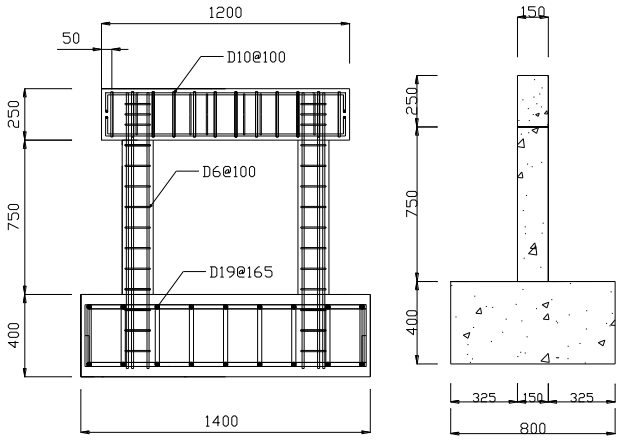

(a) Front view (b) Side view

Fig. 2 Dimensional and reinforcing details of C specimen (unit : mm)

Table 1 Detailed information of test specimens

Specimen	f_c' (MPa)	N_u (kN)	Column member					Wall member			
			$B\times D$ (mm)	ρ_v (%)	ρ_h (%)	d_{bv} (mm)	d_{bh} (mm)	$l_w\times h_w\times t_w$ (mm)	ρ_v (%)	ρ_h (%)	d_b (mm)
C	21.8	94.5	150 ×150	2.54	0.3	D10 (10)	D6 (6)	1200×1000 ×70	N.A.	0.48	D10 (10)
BC									0.71		
B		283.5									
PB		204.8						350×1000 ×70	1.09		

infill wall strengthening methods can greatly improve the lateral shear strengths of RC frames, and it also has big advantages in terms of the cost effectiveness. These methods, however, generally requires quite cumbersome construction works due to complex connection details within narrow gaps between infill wall and existing frame (i.e., a beam and columns), and also the performance of connection regions is generally vulnerable to shear, which means it is very hard to be properly controlled. To overcome such disadvantages inherent in the existing infill wall methods, this study proposed an externally-anchored precast wall panel (EPCW) method, in which the precast walls are externally anchored to the outside of the columns and beams using the pretention bolts. The EPCW method proposed in this study not only can enhance the constructability but also can reduce the construction period by utilizing a simple external anchoring system and prefabricated RC panels, respectively. In this study, cyclic loading tests were conducted to verify the proposed EPCW method with various connection details and wall sizes as the key variables.

2. Experimental investigation

2.1 Test specimens

To verify the seismic performances of RC frame structures with non-seismic details strengthened using the EPCW method, a total of four specimens were fabricated and tested, where the connection details and walls sizes were considered as the key test variables, as shown in Fig. 1 and Table 1. 1/3-scaled one bay-single story RC frames were carefully fabricated considering the capability of loading equipment in the testing laboratory. The net span length of the beam members in the existing RC frame specimens was 850 mm, and the net height of the column member was 750 mm. In the beam, D10 stirrups were placed at 100 mm spacings (i.e., D10@100 in Fig. 2). The specimen C shown in Fig. 2 was a control RC frame specimen with non-seismic details. The columns and beam dimensions were 150 mm×150 mm and 150 mm×250 mm, respectively. The specimens BC, B and PB were RC frame specimens strengthened using the EPCWs, in which all the structural details in existing RC frames before strengthening are exactly the same with the control specimen C. As shown in Fig. 3, the RC frames and precast wall panels were connected by inserting a steel rod in the perforated hole and then fastening it with a nut from the outside (i.e., from the front face) to introduce a strong compressive force. Fig. 4 shows the dimensional details of the specimen BC, in which the EPCW were integrated using the steel rods to the beams and columns of the existing RC frame structure, and the dimensions of the EPCW were 1200 mm×1000 mm×75 mm. The specimen B was fabricated with similar details to those of the specimen BC. The EPCW, however, were connected only to the beam of the existing RC frame structure using the four steel rods without any connection to the column members. Fig. 5 shows the specimen PB, in which the periphery of the columns was strengthened by two slender EPCWs, and this wing wall method has an excellent constructability and an advantage in terms of the

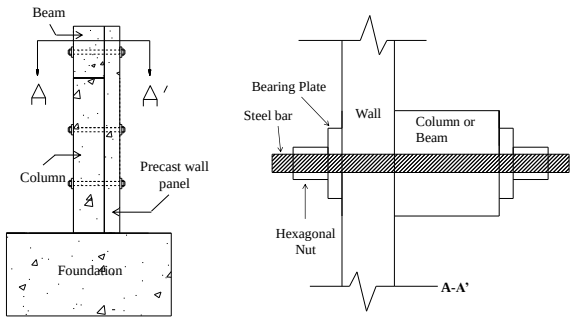

Fig. 3 Details of externally-anchored precast wall-panel connection

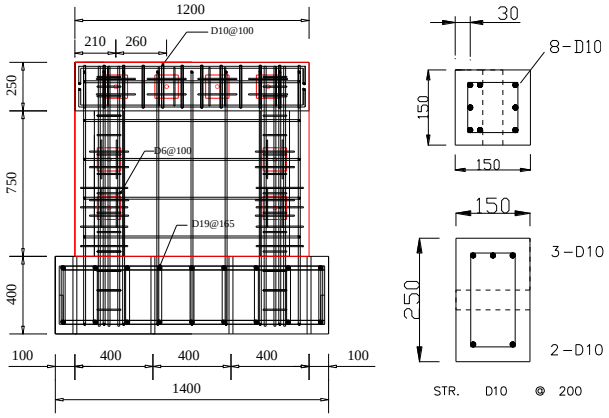

(a) Reinforcement details of specimen

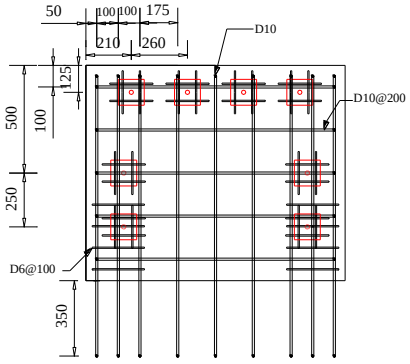

(b) Reinforcement details of wall

Fig. 4 Dimensional and reinforcing details of BC specimen (unit : mm)

architectural design to secure window spaces. The width of each slender EPCW used in the specimen PB was 350 mm, which was about 1/4 of the wall size used in the specimens BC and B. The concrete were vertically placed in the order of the foundation, column, and upper beam, which reflected the actual process of the building construction. The precast wall panels were fabricated separately from the existing RC frame structures with non-seismic details, and then the precast walls were erected and connected vertically using the dowel bars extended from the bottom edge of the EPCWs into the mechanical sleeves previously installed in the foundation of the existing RC frame structures. As shown in Figs. 4(b) and 5(b), the extended length of the dowel bars of the EPCWs was 350 mm, and the headed bars were used to prevent an anchorage failure. After finishing

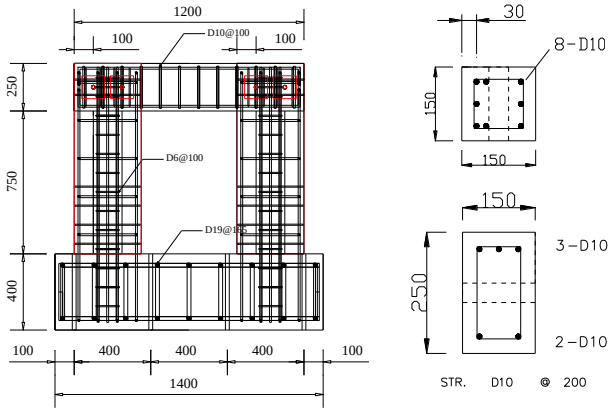

(a) Reinforcement details of specimen

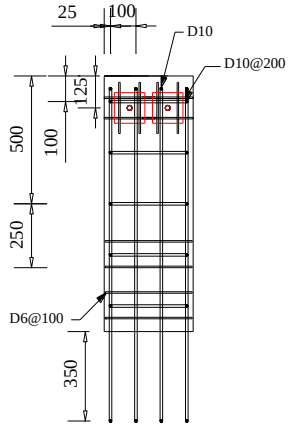

(b) Reinforcement details of wall

Fig. 5 Dimensional and reinforcing details of PB specimen (unit : mm)

connection between the EPCWs and foundation, sleeves were grouted with a non-shrinkage mortar. As shown in Fig. 3, the high-strength steel rods were used for the connection of the precast wall panel to the existing RC frame, and holes for the insertion of the steel rods and grouting holes in the columns and beams were prepared in advance. After the insertion of the steel rods inside of the holes, the nuts were fastened, and the holes were also grouted using the non-shrinkage mortar.

The material properties of the high-strength steel rods used in the external anchoring connections are summarized in Table 2, and the steel rods were assembled using hexagonal nuts and bearing plates, as shown in Fig. 3. A strain gage was attached to the center of each steel rod, and the nuts were tightened up to 300 $\mu\varepsilon$ (33.8 kN), so that the same tension forces were introduced to the steel rods. In the RC frames and EPCWs, concrete with the compressive strength of 21.0 MPa, which has been widely used for RC buildings with non-seismic details (Yun *et al*. 2006), was used. Table 3 shows the material properties of the steel reinforcements used in this study.

2.2 Test procedure

Fig. 6 shows a test set-up of the specimen installed in the loading frame. A hydraulic actuator with 1000 kN capacity was used to apply the axial load to the test

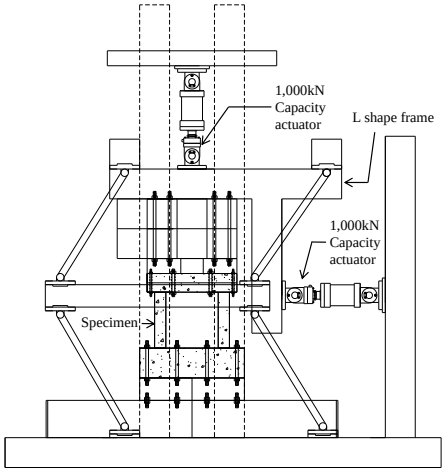

(a) Test setup

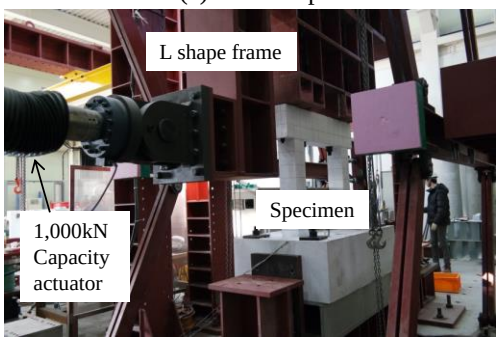

(b) Photograph of specimen setup

Fig. 6 Test set-up

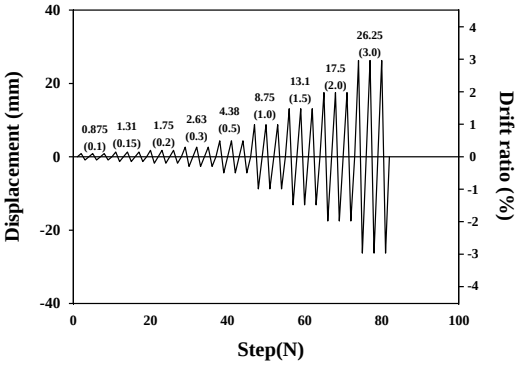

Fig. 7 Lateral cyclic loading protocols of test program

specimens, where 10.0% of the axial strength of the columns and the precast wall ($0.1A_g f_{ck}$) was constantly introduced and maintained using the load control method during testing as the gravity load (Yun *et al*. 2006). The lateral loads were applied through the displacement control method with a 1000 kN electric actuator. As shown in Fig. 7, the reversed cyclic lateral loading was applied 3 times at each drift ratio according to the target story drift profile. In addition, L-shaped and bow-shaped balance frames were utilized to ensure the actual moment and shear force distributions acting on the columns, beam and EPCWs, and five linear variable differential transformers (LVDTs) were also installed on the side of the test specimen to monitor displacement and slip behaviors. Strain gages were attached to the longitudinal reinforcements in the columns and to the

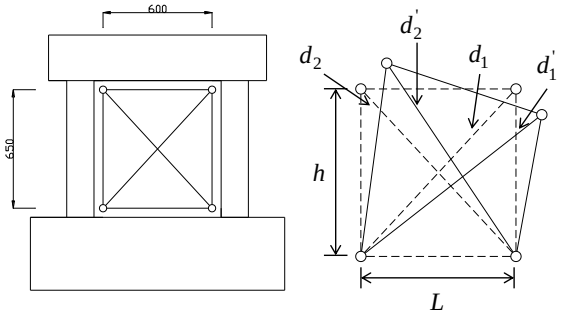

Fig. 8 nstrumentation for measuring shear distortional behaviors

Table 2 Mechanical properties of high-strength steel rod used in connections

Nominal diameter (mm)	Yield strength (MPa)	Tensile strength (MPa)	Area (mm^2)	Modulus of elasticity (MPa)
26.5	900	1,100	551	205,000

Table 3 Mechanical properties of reinforcing bars

	Yield strength (MPa)	Tensile strength (MPa)
D6	387.7	426.3
D10	501.7	619.3

vertical and horizontal reinforcements of the EPCWs, respectively. To evaluate the shear distortional deformations of the EPCWs, as shown in Fig. 8, the wire displacement transducers were attached in the specimens B and BC.

3. Experimental results

3.1 Lateral cyclic responses of test specimen

Figs. 9 and 10 show the measured lateral cyclic responses and crack patterns of the test specimens, respectively. As shown in Fig. 9(a), the maximum lateral load of the specimen C without strengthening was 54.6 kN in the positive direction and -51.7 kN in the negative direction. The maximum lateral load was observed at 1.0 % drift ratio (the ratio of the lateral displacement of story to the height of story) in both of the positive and negative directions, followed by a gradual decrease in the load responses. As shown in Fig. 10(a), for the specimen C, flexural cracks were initially observed in the upper and lower parts of the column and beam-column connection regions, at 0.15% drift ratio. As the load increased, the cracks propagated into the central regions of the column members. At 1.0% drift ratio, shear cracks occurred in the column members, and the load decreased as the crack width increased. The maximum crack width at the center of the column was measured to be 2.0 mm at 2.0% drift ratio. After the first cyclic of 2.0% drift ratio level, the concrete cover spalling was observed at the top of the column, the load was reduced to 78% of the maximum lateral load, and then test was terminated considering the stability and safety.

As shown in Fig. 9(b), the specimen BC fully

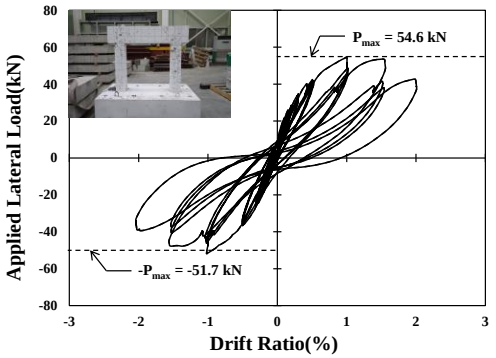

(a) Specimen C

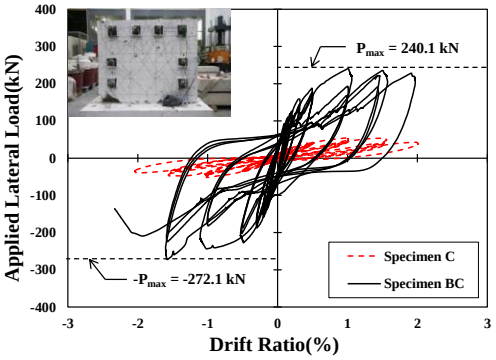

(b) Specimen BC

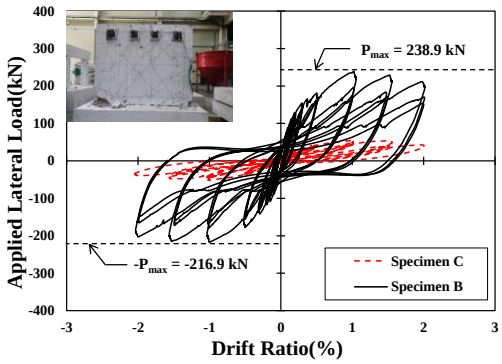

(c) Specimen B

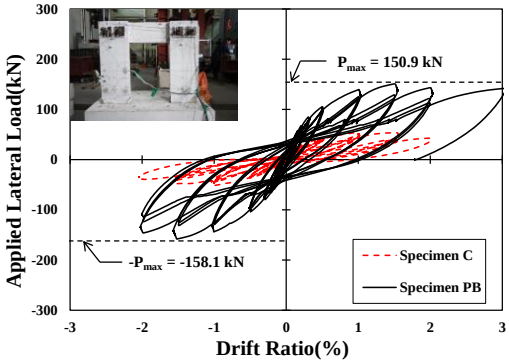

(d) Specimen PB

Fig. 9 Lateral cyclic responses of test specimens

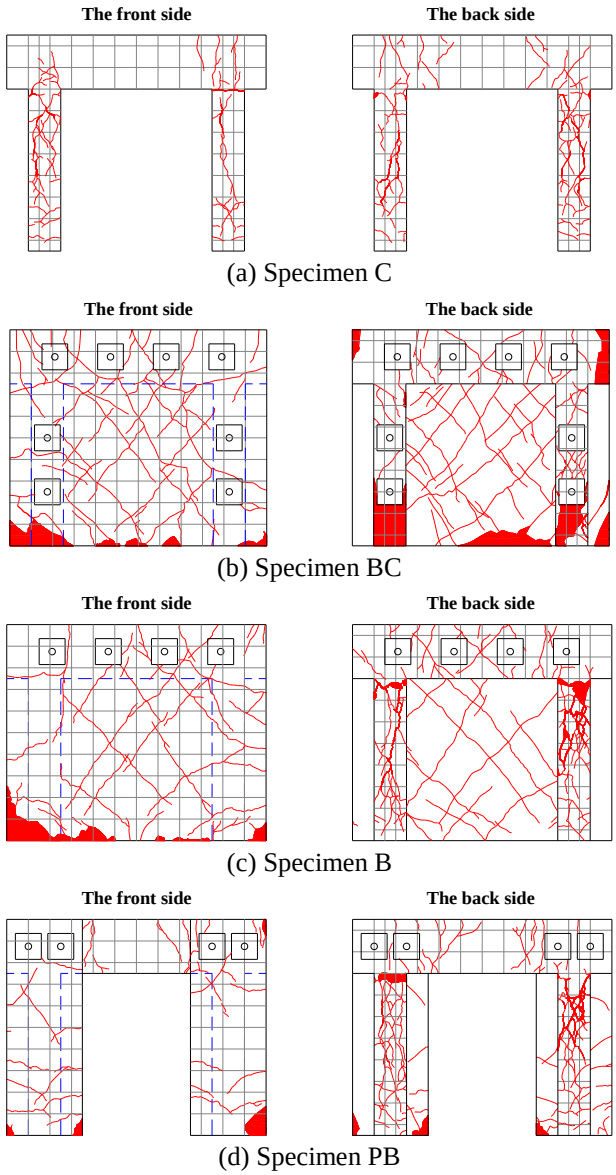

(a) Specimen C

(b) Specimen BC

(c) Specimen B

(d) Specimen PB

Fig. 10 Crack patterns of test specimens right after failure

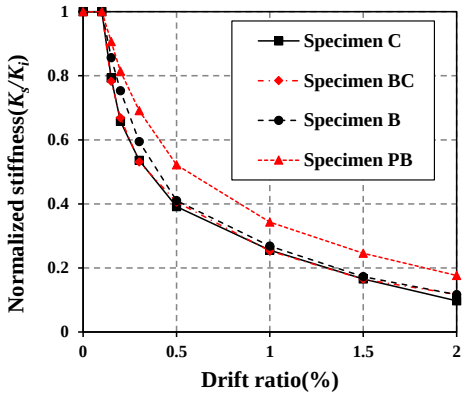

Fig. 11 Normalized stiffness depending on drift ratios

strengthened by the stocky EPCW panel, in which both the columns and beam were connected to the precast panel using the external anchoring method shown in Fig. 3, exhibited a maximum lateral load of 240.1 kN at 1.0% drift ratio and -272.1 kN at 1.5% drift ratio in the positive and negative directions, respectively. The maximum lateral loads of the specimen BC showed approximately 3.5 times and 4.2 times larger compared to those of the specimen C in the positive and negative directions, respectively. As shown in Fig. 10(b), diagonal tension cracks occurred in the

EPCW at 0.1% drift ratio, and several flexural cracks were observed in the columns at 0.2% drift ratio. In addition, multiple diagonal tension cracks were observed in the EPCW. At 1.0% drift ratio, concrete crushing at the precast wall panel-foundation connection was observed, and shear cracks were also observed in the column members. At 1.5% drift ratio, the cracks at the lower part of the column started to widen, and the spalling of the concrete covers in the column members were also observed. At this time, the maximum crack width was measured as 5.0 mm in the column and 0.7 mm in the EPCW. The specimen BC showed only 10% loading reduction at 2.0% drift ratio compared to the maximum load, and the specimen BC was failed as the load significantly decreased during the negative loading after the completion of the positive loading regime at 2.0% drift ratio.

As shown in Fig. 9(c), the specimen B strengthened by connecting the stocky EPCW only to the beam showed the maximum lateral load at 1.0% drift ratio, and the maximum lateral loads were measured to be 238.9 kN and -216.9 kN in the positive and negative directions, respectively, which were significantly enhanced lateral strength as much as 338% in the positive direction and 320% in the negative direction compared to those of the specimen C. The specimens BC and B showed slightly different behaviors in the negative direction i.e., the specimen B showed lower negative maximum strength than the specimen BC, but their overall behaviors were almost similar to each other. Flexural cracks initially occurred in the lower part of the EPCW at 0.15% drift ratio, and diagonal tension cracks were developed in the EPCW at -0.15% drift ratio. At 0.2% drift ratio, several flexural cracks were observed in the column members, and shear cracks occurred in the column members at 1.0% drift ratio, at which concrete cover spalling occurred at the precast wall panel-foundation connection. The maximum crack width was 4.0 mm in the column and 1.0 mm in the EPCW at 2.0% drift ratio, and the existing RC frame structure and the EPCW were separated from each other at the wall panel-foundation connection. The specimen B showed smaller crack widths observed in the columns, but the crack width observed in the EPCW panel was larger than the specimen BC. For the specimen B, the lateral force was reduced to 65% of the maximum lateral load in the third cycle of 2.0% drift ratio, and the testing was finally terminated after the third cyclic loading was completed at 2.0% drift ratio. As the EPCW was anchored only to the beam member in the specimen B, smaller damages were observed in the column, and more stable cyclic load behaviors were obtained compared to the specimen BC, as shown in Fig. 10(c).

As shown in Fig. 9(d), the specimen PB, in which the peripheries of the columns was strengthened using two slender wing-type EPCWs, showed a maximum lateral load of 150.9 kN in the positive direction and -158.1 kN in the negative direction at 1.5% drift ratio, respectively. The lateral strengths were 176% higher in the positive direction and 206% higher in the negative direction compared to the specimen C. The flexural cracks were observed only in the precast wall at 0.1% drift ratio. At 0.2% drift ratio, flexural cracks occurred at the top and bottom of the columns, and shear cracks were also observed in the columns at 0.5% drift ratio. The concrete spalling was initiated at the upper part of the column at 1.0% drift ratio, and the concrete at the wall-foundation connection regions was crushed at 1.5% drift ratio. At 2.0% drift ratio, the maximum crack width was observed to be 3.0 mm in the columns and 0.6 mm in the EPCW. For the specimen PB, there was no significant reduction in the lateral load even at 2.0% drift ratio, and the testing was finally terminated at 3.0% drift ratio. The specimen PB showed very stable and excellent lateral performances in that about 95% of the maximum lateral load was maintained up to 3.0% drift ratio, and less damage was accumulated to the existing RC frame structure compared to the other specimens, as shown in Fig. 10(d).

According to the existing literature, the lateral stiffness and strength can be greatly improved in the conventional infill wall methods, while it is very difficult to enhance the lateral deformation capacity or ductility. In addition, in the case that the shear strength ratio between the infill walls and the existing RC frame structure is high, the shear failure of the column members in the existing RC frame can dominate the failure mode of the RC frame structure strengthened using the infill wall. This failure mode cannot guarantee the stability of the existing RC frame structures against gravity loads, and thus it is not a desirable failure mode in the seismic strengthening (Yun *et al*. 2006, Harris *et al*. 1993, Tomazevic and Zarmic 1984). The EPCW method proposed in this study showed good lateral deformation capacities after strengthening, and all the precast walls reached their maximum strengths before the shear failures of the column members in all the test specimens. In addition, in the conventional infill wall system, the connection details are very complex to be constructed within the existing frame structures, and the performance of the entire frame structure can also be dominated by the shear performances of the connection between the infill wall and existing frame. In the proposed EPCW, as shown in Fig. 10, no significant damages were observed near the connection regions between the existing frame and EPCW due to the strong compressive forces introduced through the external anchoring system.

3.2 Stiffness degradation characteristics

Fig. 11 shows the ratio of secant stiffness (K_s) at the corresponding drift ratios to the initial stiffness (K_i) of each specimen. The specimens BC, B and C exhibited almost similar stiffness degradation characteristics. Unlike specimens BC, B and C, the specimen PB showed a lower stiffness degradation rates than the other specimens. Fig. 12 shows the comparisons of the stiffness degradation characteristics of the test specimens according to the number of the cyclic loadings at the same drift level. In the specimen C, the ratio of the stiffness of the second and third load cycles (K_{s2} and K_{s3}) to the stiffness of the first load cycle (K_{s1}) was drastically reduced after 0.5% drift ratio. This is because the shear cracks occurred in the column in the first load cycle at 0.5% drift ratio, and the load resistance performance and bond performance decreased due to the concrete damages from the following load cycles. The specimens BC and B also showed rapid stiffness degradations due to the cyclic loading after 0.5% drift ratio,

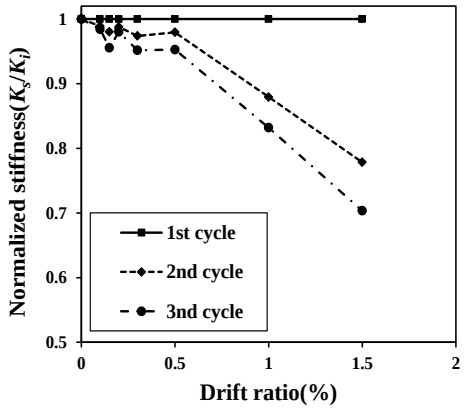

(a) Specimen C

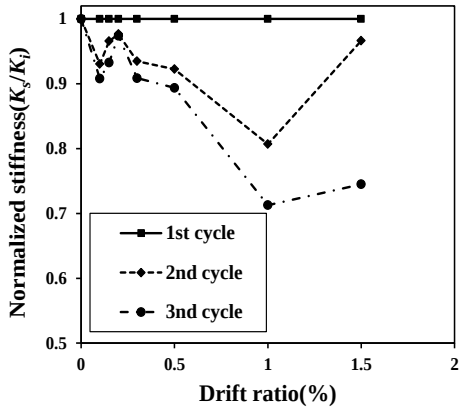

(b) Specimen BC

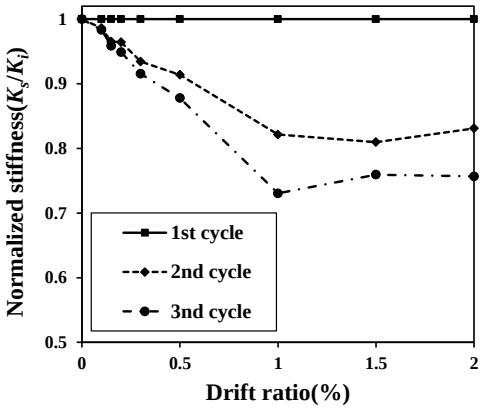

(c) Specimen B

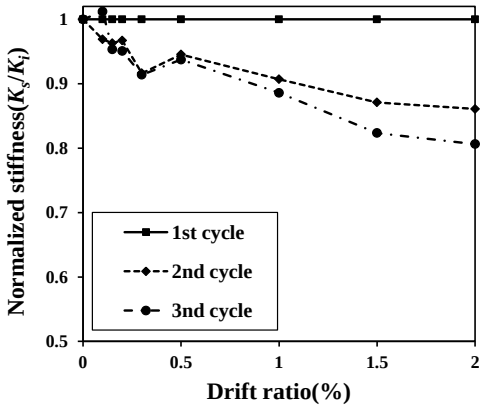

(d) Specimen PB

Fig. 12 Stiffness degradation behaviors of test specimens due to repeated loadings

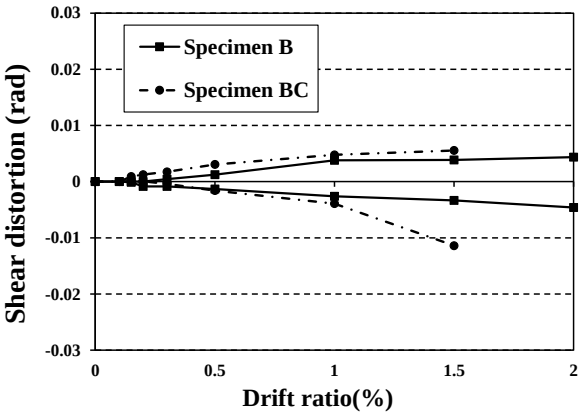

Fig. 13 Comparison of measured shear distortions of test specimens

where the shear cracks of the column were observed. The specimen PB exhibited similar stiffness degradation characteristics up to 1.0% drift ratio, but it appeared that the stiffness degradations caused by the cyclic loading were less severe than those observed in the other specimens after 1.0% drift ratio.

3.3 Shear distortions of precast wall

The shear force is mainly resisted in a conventional RC wall by the compressive strut action. The load-carrying capacity of the concrete compressive struts decreases when the cracks propagate into the concrete strut areas in the RC walls subjected to cyclic loadings. In consequence, the shear stiffness of the walls decreases, which induces large shear distortions in the RC shear wall (Sittipunt *et al*. 2001). Fig. 13 shows a comparison of the average shear strain calculated using the measured data from the specimens B and BC at each drift ratio, where the average shear strain (γ_{avg}) was estimated based on Oesterle *et al*. (1976), as follows

$$\gamma_{avg} = \frac{\left(d_1^{'} - d_1\right)d_1 - \left(d_2^{'} - d_2\right)d_2}{2hL} \quad (1)$$

The specimens B and BC showed similar shear strain up to 1.0% drift ratio, but it can be confirmed that the shear strain of the specimen BC increased sharply at 1.5% drift ratio compared to that of the specimen B. Although the same EPCWs were adopted in both the specimens B and BC, the test results were quite different. This indicates that, in the specimen BC, the external anchoring connections were also provided in the columns and beam with the EPCW, and, therefore, a large amount of damage was inevitably accumulated in the column members, as shown in Fig. 10. In addition, this column damage was occurred at an earlier stage for the specimen BC compared to the specimen B, and thus the shear contributions of the EPCW would be higher in the specimen BC, and thus the large distortional deformations were observed in the specimen BC.

3.4 Energy dissipation capacities of test specimens

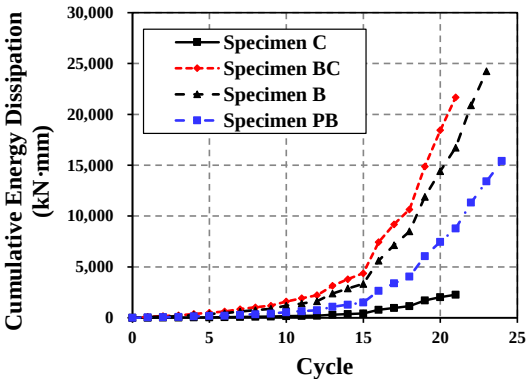

Fig. 14 Energy dissipation characteristics of test specimens

The structure should possess proper energy dissipation mechanisms to ensure that the system has sufficient seismic performances. Therefore, the cumulative energy dissipation serves as an important index in the seismic performance evaluations (Ozden *et al*. 2011). Fig. 14 shows the cumulative energy dissipation of each test specimen with respect to the number of the loading cycles. In this study, the cumulative energy dissipation was defined as the closed area of the load-displacement hysteresis curve, as shown in Fig. 10. It appeared that the specimen BC dissipated more energy at the same loading cycle than the specimen B. This is because the specimen BC showed higher lateral capacity in the negative loading direction. The amount of the final cumulative energy dissipation, however, was larger in the specimen B, because the testing was terminated for the specimen BC with a decrease in the load-bearing capacity during the loading in the negative direction at 2.0% drift ratio. At the third cycle at 1.5% drift ratio, the amount of the cumulative energy dissipation of the specimen C was estimated to be 2,267 kN·mm, and those of the specimens BC, B and PB were 21,685, 16,732, and 8,777 kN·mm, which were 956%, 738%, and 387% higher values than the specimen C, respectively.

3.5 Strain behaviors of test specimens

Fig. 15 and Table 4 show the strain behaviors of the longitudinal reinforcements in the columns of the test specimens. The specimen C showed the maximum strains of 2047 $\mu\varepsilon$ and -2147 $\mu\varepsilon$ in the positive and negative directions, respectively. And it can be confirmed that the longitudinal reinforcements in the RC frame columns reached their yield strains. The specimen BC showed the maximum strains of 1200 $\mu\varepsilon$ and -1367 $\mu\varepsilon$ in the positive and negative directions, respectively. In addition, the maximum strains were 1695 $\mu\varepsilon$ and -2567 $\mu\varepsilon$ for the specimen B and 2151 $\mu\varepsilon$ and -2473 $\mu\varepsilon$ for the specimen PB, respectively. In the case of the specimen B, as the EPCW was connected only to the beam, the column showed the conventional flexure-dominated behavior. The specimen BC, however, showed the shear-dominant behavior due to strong anchoring connections between the column and EPCW, and thus the strains of the longitudinal reinforcement of the column was measured smaller than those of the specimen B.

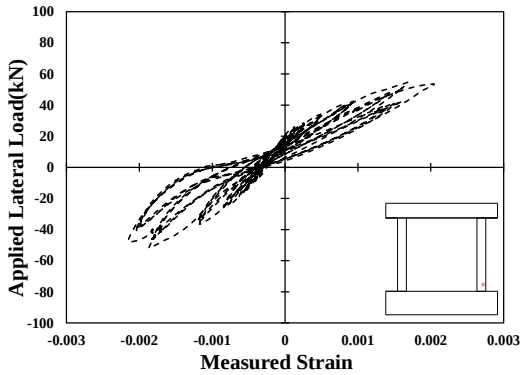

(a) Specimen C

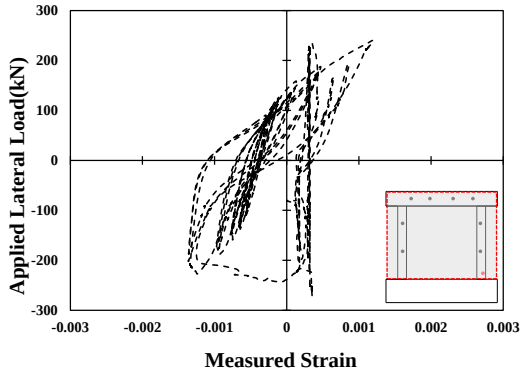

(b) Specimen BC

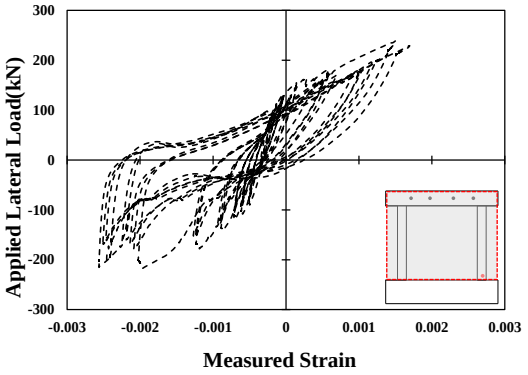

(c) Specimen B

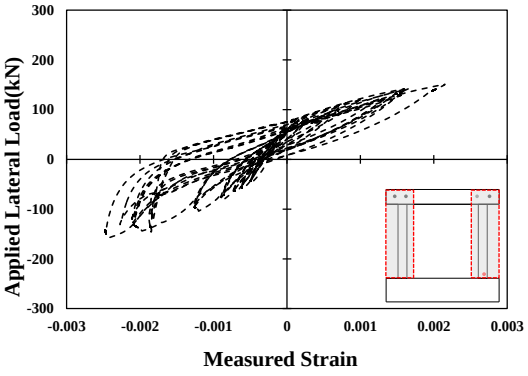

(d) Specimen PB

Fig. 15 Measured strain behaviors of vertical reinforcement in column members

Figs. 16 and 17 show the strain behaviors measured from the vertical and horizontal reinforcements in the EPCWs of the test specimens, respectively. No large strains

Table 4 Maximum strains of specimens

	Positive direction ($\mu\varepsilon$)	Negative direction($\mu\varepsilon$)
C	2047	-2147
BC	1200	-1367
B	1695	-2567
PB	2151	-2473

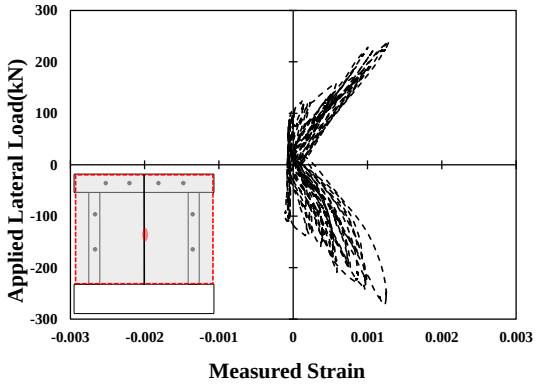

(a) Specimen BC

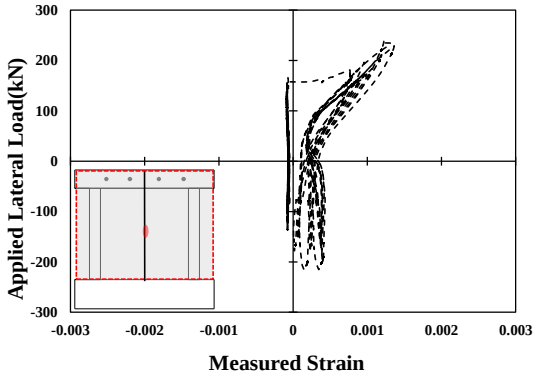

(b) Specimen B

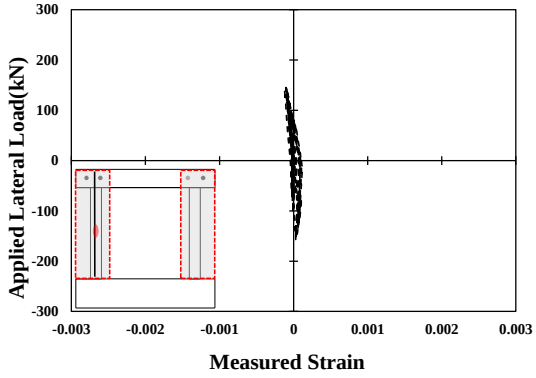

(c) Specimen PB

Fig. 16 Measured strain behaviors of vertical reinforcement in precast wall panel

were observed in the reinforcements placed in the vertical and horizontal directions, but higher strains were observed in the horizontal reinforcement than those in the vertical reinforcement. In this study, as shown in Fig. 6, since the L-shaped and bow-shaped balance frames were introduced, the EPCWs behaved predominantly in shear as intended, and relatively small vertical strain was developed due to flexure. For the specimen PB, the maximum strains in the

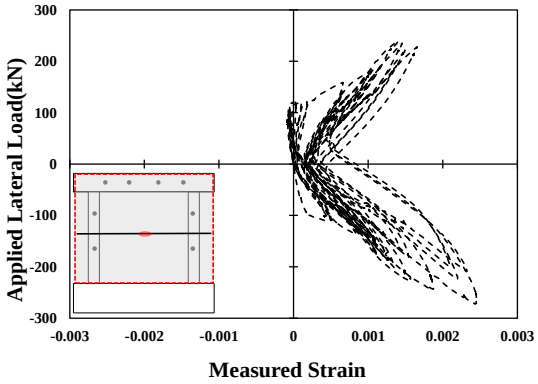

(a) Specimen BC

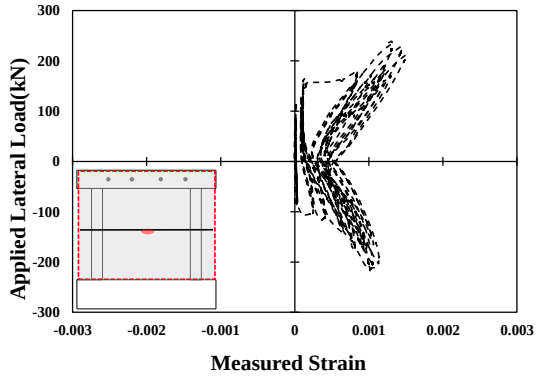

(b) Specimen B

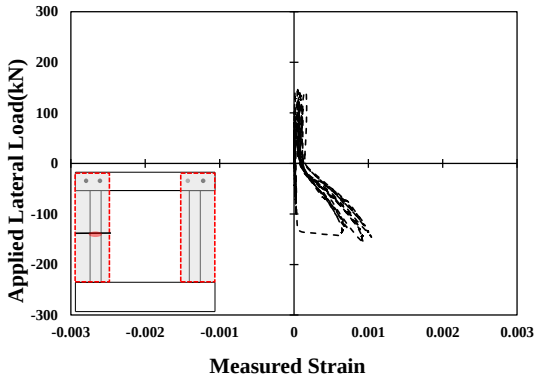

(c) Specimen PB

Fig. 17 Measured strain behaviors of horizontal reinforcement in precast wall panel

vertical and horizontal reinforcements were measured as 100 $\mu\varepsilon$ and 1040 $\mu\varepsilon$, and those of the specimen BC were measured to be 1300 $\mu\varepsilon$ and 2450 $\mu\varepsilon$, respectively. In the case of the specimen BC, the large strain was observed in the horizontal reinforcement during the negative loading compared to that of the vertical reinforcement, and this is because the horizontal reinforcements in the EPCW yielded as the shear contribution of the EPCW increased after the columns were severely damaged due to the cyclic loadings. In the case of the specimen B, the maximum strain of the vertical reinforcement was 1350 $\mu\varepsilon$ and that of the horizontal reinforcement was 1500 $\mu\varepsilon$, which are quite small strains compared to the specimen BC. This indicates that the shear contribution of the EPCW in the specimen BC was higher than that of the specimen B as the accumulated damages to the existing RC frame structure in the specimen

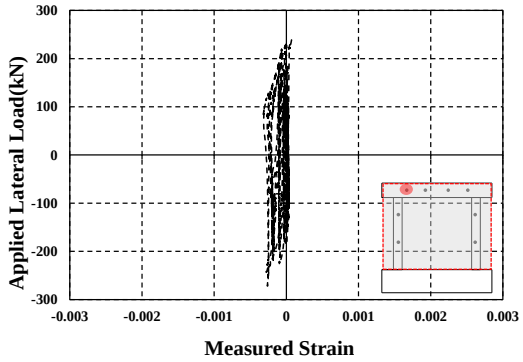

(a) Steel rods in the beam

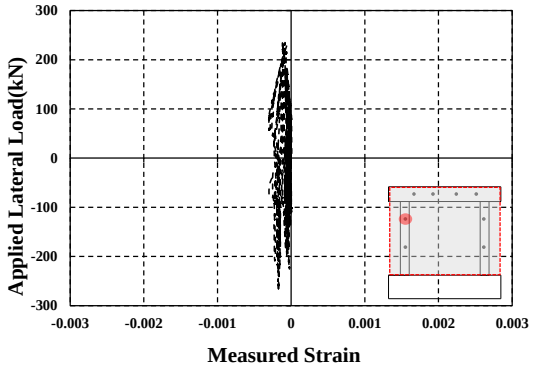

(b) Steel rods in the column

Fig. 18 Measured strain behaviors of steel rods in specimen BC

BC was larger than that in the specimen B, which is also consistent results with those explained in Fig. 13. Strain behaviors measured from steel rods in the specimen BC are shown in Fig. 18. Strain gages were attached to the center of each steel rods, and measured during the test. The strain of steel rods measured in the test was found to be approximately 200~300 $\mu\varepsilon$.

4. Conclusions

This study proposed the externally anchored precast wall panel (EPCW) method to overcome the limitations in the conventional infill wall methods. The RC one bay-single story frame test specimens with and without strengthening were fabricated, and the lateral cyclic loading tests were conducted to verify the proposed method. On this basis, following conclusions were obtained:

1) The specimens BC and B strengthened using the EPCWs showed about 3 times higher lateral strengths and almost equal deformation capacity compared to the specimen C with non-seismic details.

2) The lateral strength of the specimen PB, in which the peripheries of the columns was strengthened by two slender wing-type EPCWs, was about 1.5 times higher than that of the specimen C without strengthening. In addition, the specimen PB showed the stable cyclic behavior up to 3.0% drift ratio, which shows enhanced deformation capacity of the specimen PB compared to other specimens.

3) It is considered that the wing-type slender EPCWs can enhance the lateral strength and stiffness, and it is also advantageous in the constructability and architectural flexibility.

4) The RC frame specimens strengthened using the EPCWs showed less structural damages in the column members of the existing frame structures with non-seismic details, thus showing a more stable lateral behavior. In particular, the application of the anchoring connection to the beam member only is expected to be more advantageous than the connections of both the beam and the columns in terms of the constructability and seismic performances.

5) The EPCW strengthening method proposed in this study can be applicable to existing RC frame structures for seismic reinforcement.

Acknowledgments

This research was supported by Mid-career Researcher Program through the National Research Foundation of Korea (NRF) funded by the Ministry of Education, Science and Technology (2016R1A2B2010277).

References

Almusallam, T.H. and Al-Salloum, Y.A. (2007), "Behavior of FRP strengthened infill walls under in-plane seismic loading", *J. Compos. Constr.*, **11**(3), 308-318.

Bailey, C.G. and Yaqub, M. (2012), "Seismic strengthening of shear critical post-heated circular concrete columns wrapped with FRP composite jackets", *Compos. Struct.*, **94**(3), 851-864.

Baran, M. and Tankut, T. (2011), "Experimental study on seismic strengthening of reinforced concrete frames by precast concrete panels", *ACI Struct. J.*, **108**(2), 227-237.

Bas, S., Lee, J.H., Sevinc, M. and Kalkan, I. (2017), "Seismic performance of R/C strctures under vertical ground motion", *Comput. Concrete*, **20**(4), 369-380.

Frosch, R.J. (1996), "Panel connections for precast concrete infill walls", *ACI Struct. J.*, **96**(4), 467-472.

Frosch, R.J. (1996), "Seismic rehabilitation using precast infill walls", PhD Thesis, Department of Civil Engineering, the University of Texas at Austin, Austin, TX.

Harris, H.G., Ballouz, G.R. and Kopatz, K.W. (1993), "Preliminary studies in seismic retrofitting of lightly reinforced concrete frames using masonry infills", *Proceeding of the 6th North American Masonry Conference*, Masonry Society, 383-395

Kabeyasawa, T., Toshikazu, K., Kim, Y.S., Kabeyasawa, T. and Bae, K.K. (2009), "Tests on reinforced concrete columns with walls for hyper-earthquake resistant system", *Proceedings of the 3rd International Conference on Advanced in Experimental Structural Engineering*, October.

Kahn, L.F. and Hanson, R.D. (1979), "Infilled walls for earthquake strengthening", *J. Struct. Div.*, **105**(2), 283-296.

Karaca, Z., Türkeli, E. and Pergel, Ş. (2017), "Seismic assessment of historical masonry strctures: The case of Amasya Taşhan", *Comput. Concrete*, **20**(4), 409-418.

Karantoni, F.V. (2013), "Seismic retrofitting of Fragavilla Monastery", *Earthq. Struct.*, **5**(2), 207-223.

Kim, S.W., Yun, H.D. and Jang, Y.H. (2009), "Structural performance of precast infill walls as a damage-fuse element for

seismic retrofit", *J. Arch. Inst. Kor.*, **25**(3), 43-50.
Koutas, L., Bousias, S.N. and Triantafillou, T.C. (2015), "Seismic strengthening of masonry-infilled RC frames with TRM: Experimental study", *J. Compos. Constr*., **19**(2), 1-12.
Lee, H.S., Lee, H.B., Hwang, K.R. and Cho, C.S. (2013), "Shake table responses of an RC low-rise building model strengthened with buckling restrained braces at ground story", *Earthq. Struct.*, **5**(6), 703-731.
Lee, K.S., Wi, J.D., Kim, Y.I. and Lee, H.H. (2009), "Seismic safety evaluation of Korean R/C school buildings built in the 1980s", *J. Kor. Concrete Inst.*, **13**(5), 1-11.
Lin, W., Wang, Q., Li, J., Chen, S. and Qi, A. (2017), "Shaking table test of Pounding Tuned Mass Damper (PTMD) on a frame structure under earthqauke excitation", *Comput. Concrete*, **20**(5), 545-553.
Matsumoto, T. (1998), "Structural performance of SC multi-story shear walls with infilled precast concrete panels", *JPN Concrete Inst.*, **20**(1), 187-194.
Meshaly, M.E., Yoissef, M.A. and Abou Elfath, H.M. (2014), "Use of SMA bars to enhance the seismic performance of SMA braced RC frames", *Earthq. Struct.*, **6**(3), 267-280.
Ministry of Education (MOE) and Korea Institute of Educational Environment (KIEE) (2011), "Guideline for seismic evaluation and rehabilitation of exsting school buildings in Korea", 1-108. (in Korean)
Motezaker, M. and Kolahchi, R. (2017), "Seismic response of concrete columns with nanofiber reinforced polymer layer", *Comput. Concrete*, **20**(3), 361-368.
Oesterle, R.G., Fiorato, A.E., Johal, L.S., Carpenter, J.E., Russell, H.G. and Corley, W.G. (1976), "Earthquake resistant structural walls-Tests of isolated walls", Report to National Science Foundation, Construction Technology Laboratories, Portland Cement Association, Skokie, III, October.
Ozden, S., Akguzel, U. and Ozturan, T. (2011), "Seismic strengthening of infilled reinforced concrete frames with composite materials", *ACI Struct. J.*, **108**(4), 414-422.
Sahoo, D.R. and Rai, D.C. (2010), "Seismic strengthening of non-ductile reinforced concrete frames using aluminum shear links as energy-dissipation devices", *Eng. Struct.*, **32**(11), 3548-3557.
Sittipunt, C., Wood, S.L., Lukkunaprasit, P. and Pattararattanakul, P. (2001), "Cyclic behavior of reinforced concrete structural walls with diagonal web reinforcement", *ACI Struct. J.*, **98**(4), 554-562.
Tesser, L. and Talledo, D.A. (2017), "Efficient membrane element for cyclic response of RC panels", *Comput. Concrete*, **20**(3), 351-360.
Tomazevic, M. and Zarnic, R. (1984), "The behaviour of horizontally reinforced masonry walls subjected to cyclic lateral in-plane reversals", *Proceeding of the 8th European Conference on Earthquake Engineering*, **4**(1), 1-8.
Yun, H.D., Kim, S.W., Lee, K.W., Choi, C.S. and Lee, H.Y. (2006), "Seismic performance of lightly reinforced concrete frames with high performance fiber-reinforced cement composite infill walls", *J. Arch. Inst. Kor.*, **22**(5), 31-38.

CC